



Université Mohamed Khider de Biskra
Faculté des Sciences Exactes, des Sciences de la Nature et
de la Vie
Département de Science de la Matière

MÉMOIRE DE MASTER

Science de la Matière
Physique
Science des Matériaux

Réf. :

Présenté et soutenu par :
Ben Yahia Ali
Zeraib Abdelkhaliq

Le :

Study the effect of concentration
on the physical properties of the
elaborated MgO-ZnO thin film

Jury :

Dr. BENRAMACHE Said Professeur Université de Biskra Rapporteur

Année universitaire : 2020-2021

Sommaire

	General Introduction	04
	Chapter I: MgO-ZnO Thin Film	
I.1	Introduction	06
I.2	Definition of thin layer	06
I.3	MgO thin films	07
I.4	ZnO thin films	09
I.5	The thin films alloys	13
I.6	Elaboration methods of MgO-ZnO thin film	14
I.7	Applications	17
I.8	Conclusion	18
	References	18
	Chapter II Experimental Section	
II.1	Introduction	24
II.2	Elaboration	24
II.3	Spray pyrolysis technique (SPT)	24
II.4	The advantages of the spray pyrolysis technique	25
II.5	Experimental procedure	25
II.6	Thin Film Deposition	29
II.7	Conclusion	33
	References	33
	Chapter III Results and discussion	
III.1	Introduction	36
III.2	Experimental procedure	36
III.3	The structural characterizations	37
III.4	The Optical characterizations	41
III.5	Conclusion	45
	References	45
	General Conclusion	48

GENERAL

INTRODUCTION

General introduction

Mixed metal oxides have found increasing research focus and applications in physics, chemistry, materials science and engineering. The combination of two or more metals in an oxide matrix can produce materials with novel physical and chemical properties leading to relatively higher performance in various technological applications. During the last few years, synthesis of metal oxide nanocomposite materials have been attracted considerable attention. The metal oxides nanocomposites are extremely important technological materials for use in optoelectronic and photonic devices and as catalysts in chemical industries. Zinc oxide (ZnO) is a wide band gap n-type semiconductor with an energy gap of 3.37 eV at room temperature. It has been used considerably for its catalytic, electrical, optoelectronic, and photochemical properties.

MgO is typical wide band gap semiconductor; it possesses unique optical, electronic, magnetic, thermal, mechanical and chemical properties due to its characteristic structures. These two oxides have been widely used in almost the same application areas. Developing a new composite material by combining them into one could open up a new direction for research and applications. In recent years, researchers have focused more on the synthesis of nanocomposite of ZnO/ MgO due to their application in advanced technologies. Various physicochemical techniques have been employed to construct nanosized ZnO/MgO nanoparticles.

Several techniques have been also developed to prepare nanocomposite of ZnO/MgO. This nanocomposite has attracted much attention because it has a larger band gap than ZnO. However, most of the techniques need high temperatures and perform under a costly inert atmosphere. Our goal in this research is to suggest an easy method to synthesize zinc oxide/magnesium oxide nanocomposite. Considering the importance of luminescent materials in interdisciplinary materials science and future optoelectronic applications, the present work is focused on the synthesis of zinc oxide/magnesium oxide (ZnO/MgO) nanocomposites. They have attracted increasing interest in fabricating nanostructures with the size and the optical properties could be achieved by varying the solvents. With this motivation, ZnO/MgO nanocomposites were prepared by simple precipitation process and their structural, size and optical properties were studied. The as-synthesized samples are subjected to the different characterization techniques such as the powder X-Ray Diffraction (XRD), the Fourier Transform Infrared (FTIR), the Ultraviolet-visible (UV-vis) absorption and the Photoluminescence (PL) analyzes.

Chapter I:

MgO-ZnO Thin Film

I.1 Introduction

Several studies has been reported on the processing of magnesia thin films over the past few decades [1,2,3], as many fruitful advances in thin film deposition technique have occurred. The formation of thin films depends on many parameters including deposition technique due to their structure and properties [4, 5]. Among the factors which determine the physical, electrical, optical and other properties of a film we cite for example rate of deposition, environmental conditions, substrate temperature, presence of foreign matter in the deposit or its purity and inhomogeneity of the film. Various deposition methods have been used to understand the influence of these parameters on the formation of MgO-ZnO thin films [4, 6].

In this chapter we report the definition of the thin layer, MgO-ZnO thin films and its main alloys as well as some elaboration methods and finishing with some applications in different fields.

I.2 Definition of thin layer

A thin layer of a given material is an element of this material which its thickness has been greatly reduced to the Angstrom Å scale and this small distance between the two limits (almost two dimensional), in general, causes instability and degradation over time [7]

The essential difference between the material in the bulk state and the thin layer state is related to the fact that in the massive state we usually neglect, with reason, the roles of the boundaries in the properties, whereas in a thin layer these are at contrary the effects related to the surface that are preponderant. It's pretty obvious that the lower the thickness, the more this bidimensionality effect will be important. Conversely, when the thickness of a thin layer exceeds a certain threshold, the thickness effect will become minimal and the material will regain the well-known properties [8].

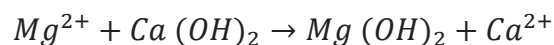
The second essential characteristic of thin layer is that, whatever the procedure used for its fabrication, a thin layer is always built on a support (although sometimes it is separated of the support). Consequently it will be imperative to take into account this major fact in the design, namely that the support has a very strong influence on the structural properties of the

deposited layer. So a thin layer of a same material and same thickness may have significant difference depending on whether it will be deposited on an amorphous insulating substrate such as glass or a monocrystalline silicon substrate for example. Consequently to these characteristics, thin layer is anisotropic by construction.

In practice we can distinguish two main families of methods, those that use a carrier gas to move the deposited material from a container to the substrate and which are similar to the diffusion techniques used in manufacturing active compounds, and those that involve a very low pressure environment and in which the material to be deposited will be conveyed by means of an initial pulse of thermal or mechanical nature [9].

I.3 MgO thin films

Magnesium oxide is produced by the calcination of magnesium carbonate or magnesium hydroxide. The latter is obtained by the treatment of magnesium chloride solutions, typically seawater, with lime [10].



Calcining at different temperatures produces magnesium oxide of different reactivity. High temperatures 1500 – 2000 °C diminish the available surface area and produces dead-burned (often called dead burnt) magnesia, an unreactive form used as a refractory. Calcining temperatures 1000 – 1500 °C produce hard-burned magnesia, which has limited reactivity and calcining at lower temperature, (700–1000 °C) produces light-burned magnesia, a reactive form, also known as caustic calcined magnesia. Although some decomposition of the carbonate to oxide occurs at temperatures below 700 °C, the resulting materials appear to reabsorb carbon dioxide from the air [11].

The use of MgO, With a low dielectric loss, shows a wide application in semiconductor systems. In addition, due to its low refractive index ($n = 1.7$), MgO is especially suitable as a buffer for epitaxial optical waveguide films [12]. Moreover, textured MgO thin films could provide a possible template for epitaxial growth of textured perovskite oxides. However, in spite of its growing relevance in science and technology, the understanding and control of the growth process of MgO thin films are limited so far,

especially the strain relaxation process. Strain relaxation in MgO thin films plays a pronounced role in influencing the crystal quality and subsequent performance in devices.

The structure assigned to MgO can be regarded as a cubic close packing of O^- ion and all the octahedral sites are filled with Mg^+ ions (**Fig. I.1**). Each O^- ion is surrounded by six Mg^+ ions and each Mg^+ ions is surrounded by six O^- ions to produce 1:1 co-ordination. The radius ratio falls within the range of $0.41-0.73 A^\circ$, which is the radius ratio of stable octahedral coordination. Existing high bond strength in ionic crystal is due to the strong electrostatic forces between ions and hence MgO an ionic crystal, exhibits hardness and high melting point and low electrical conductivity. Its structural, physical, optical and electronic properties are listed in **Table I.1**.

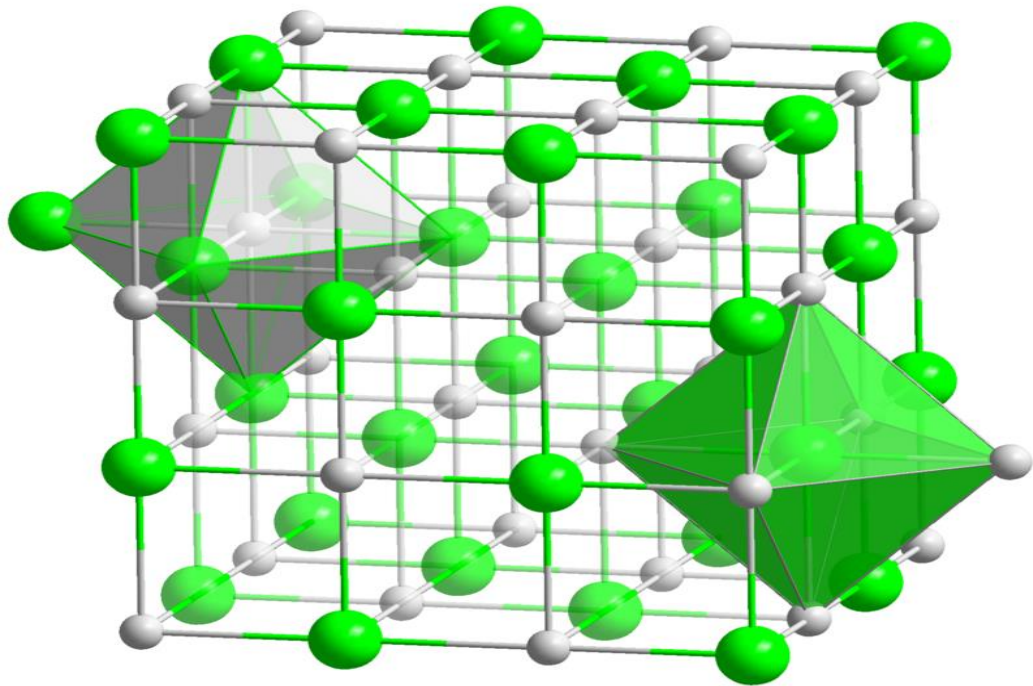


Fig I.1: MgO crystal structure.

Table I.1: Summary of Material properties of MgO [13]

Property	Parameters	values
Physical	Crystal type	Cubic
	Density	3.85 g/cm ³
	Melting Point	2800 °C
	Boiling point	3600°C
Chemical	Color	White
	Chemical formula	MgO
	Molecular weight	40.304 g/mol
	Number of atoms /cm ²	2×10 ²³
Optical	Optical band gap eV	7.2
	Absorption coefficient/cm (2μm)	0.05
Dielectric	Dielectric constant	9.8
	Refractive index	1.739

I.4 ZnO thin films

Zinc oxide

Zinc Oxide is a II - VI compound semiconductor. It exists in natural form, under the name of "Zincite", but can also be synthesized artificially in solid form "ZnO bulk" with different colors depending to the impurities that it contains (Fig.I.2) [22].

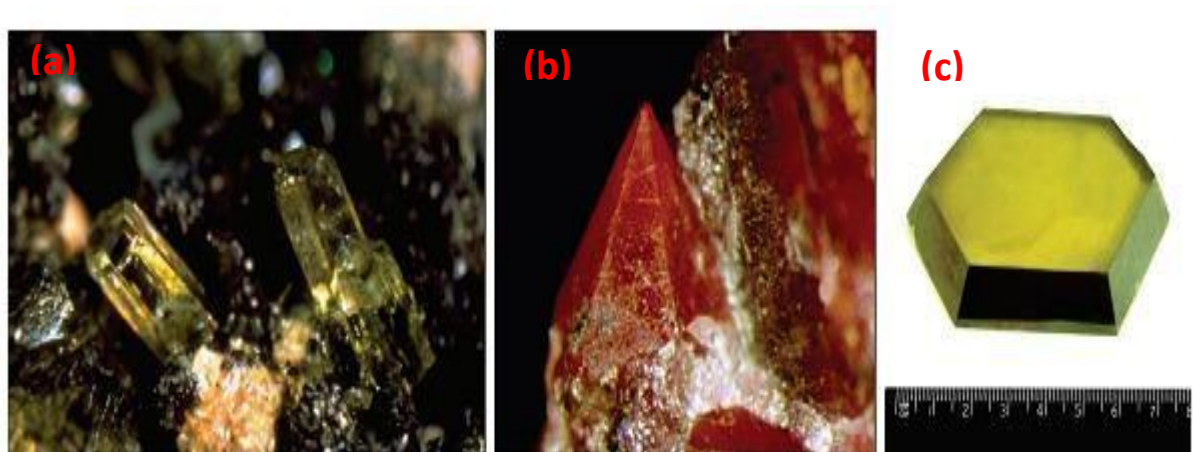


Fig.I.2. ZnO bulk in natural form (a) and (b) and from hydrothermal synthesis (c).

Most of the group II–VI binary compound semiconductors crystallize in either cubic zinc blende or hexagonal wurtzite (Wz) structure where each anion is surrounded by four cations at the corners of a tetrahedron, and vice versa. This tetrahedral coordination is typical of sp^3 covalent bonding nature; but these materials also have substantial ionic character that tends to increase the band gap beyond the one expected from the covalent bonding [23].

I.4.1 Structural properties

ZnO has a hexagonal close packing (HCP) structure called wurtzite. The structure of ZnO consists of alternating planes composed of O^{2-} and Zn^{2+} ions, which are tetrahedrally coordinated and stacked along the c-axis on an alternate basis (Fig. I.3). In addition, there are other structures such as cubic zinc blende and rock salt. Among them, wurtzite structure is the most common ZnO phase at ambient pressure and temperature [24]. The zinc oxygen bond length is 0.1992 nm parallel to the c - axis and 0.1973 nm in the other three directions of the tetrahedral arrangement of nearest neighbours [25]

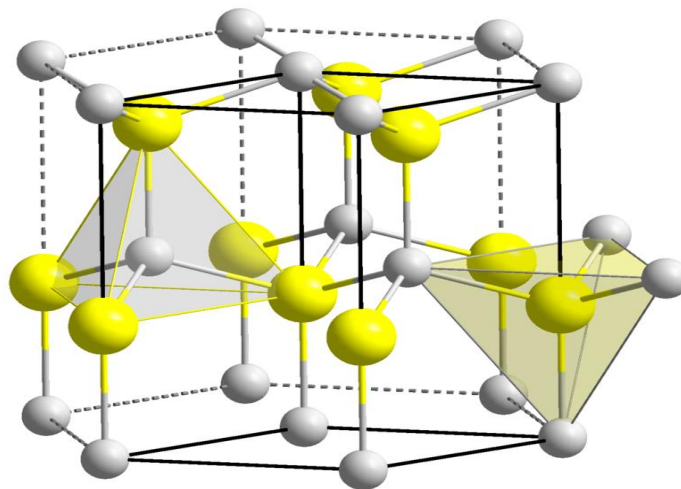


Fig.I.3 ZnO unit cell (hexagonal close packing (HCP) structure type wurtzite).

The unit cell parameters consist **a** and **c** which $a = 0.325$ nm and $c = 0.5206$ nm.

In order to describe zinc oxide, hexagonal indices can be used based on a four-coordinate system with indices $(hkil)$. This is more suitable for zinc oxide than the three coordinate system because of the source of possible confusion in assigning planes when equivalent planes

do not have the same indices. Possible confusion is avoided' using the four coordinate system as equivalent planes are indicated by permutations of the first three indices.

For example the three main reflections from the XRD spectrum of a polycrystalline powder sample of zinc oxide using the three coordinate system (hkl) are the (100), (101), and the (002) planes. Under the four coordinate system the labels are the (1010), The (1011) and the (0002). Note that (110) is not equivalent to (101) in the hexagonal Structure and this is explicit in the 4 coordinate system where these planes become

(1120) and (1011) respectively. The following formula is used to convert from three to four indices [25].

$$i = -(h + k) \quad (I. 1)$$

Another important characteristic of ZnO is polar surfaces. The most common polar surface is the basal plane. The oppositely charged ions produce positively charged Zn-(0001) and negatively charged O (0001) surfaces, resulting in a normal dipole moment and spontaneous polarization along the c-axis as well as a divergence in surface energy. To maintain a stable structure, The polar surfaces generally have facets or exhibit massive surface reconstructions, but ZnO \pm (0001) are exceptions :they are atomically flat, stable and without reconstruction[26.27].

The internal stress in ZnO thin films is given by the following relationship:

$$\sigma = \left[\frac{2c_{13}^2 - (c_{11} + c_{12})c_{33}}{c_{13}} \right] \left(\frac{c_{\text{Film}} - c_{\text{bulk}}}{c_{\text{bulk}}} \right)$$

Where, c_{bulk} is the unstrained lattice parameter of ZnO equals to 0.5206 nm, c_{film} is the lattice parameter of the strained films calculated from X-ray diffraction data and $C_{11} = 209.7$ GPa, $C_{12} = 121.1$ GPa, $C_{13} = 105.1$ GPa and $C_{33} = 210.9$ GPa are the stiffness constants of bulk ZnO[28].

I.4.2 Optical properties

The important optical properties of ZnO thin

- film are: Transmission, T
- Reflection,
- R
- Absorption
- , A
- Refraction
- Index, n
- Extinction
- Coefficient
- , k Band
- Gap, E_g
- Geometry

Geometry is an extrinsic property which encompasses the physical attributes of the film, including thickness, uniformity and surface roughness.

Transmission, reflection and absorption are intrinsic properties of the film dependant on the chemical composition; they are determined by the resultant two properties refractive index, extinction, band gap and geometry. The properties of ZnO that differentiate it from other semiconductors or oxides or render it useful in many applications:

- Large exciton binding energy: ZnO has some significant advantages in its large free exciton binding energy (60 meV compared to 21-25 meV for GaN) [15, 16], that allows for efficient excitonic emission in ZnO can persist at room temperature and higher [15].

Since the oscillator strength of excitons is typically much larger than that of direct electron-hole transitions in direct gap semiconductors [17], the large exciton binding energy makes ZnO a promising material for optical devices that are based on excitonic effects.

- Direct and wide band gap : ZnO has a band gap of 3.44 eV at low temperatures and 3.37 eV at room temperature [18], which corresponds to emission in the UV region. This band gap is very close to that of GaN (3.39eV), and GaN has been the subject of much research over the past years, even being incorporated into the recent Blu-Ray drives. For comparison, the respective values for wurtzite GaN are 3.50 eV and 3.44 eV [19]. this enables applications in optoelectronics in the blue UV region, including laser diodes,

light-emitting diodes and photodetectors [20,21]. Optically pumped lasing has been reported in ZnO platelets [15], thin films [16], ZnO nanowires [22] and clusters consisting of ZnO nanocrystals [23]. Recently a many of reports on p–n homojunctions have appeared [24,25,26], but stability and reproducibility have not been established.

I.4.3 Electrical properties

As-grown ZnO has always been found to be n-type. It was always assumed that the dominant donor was either oxygen vacancy V_O , or the zinc interstitial Zn_i , since most sample are grown under Zn-rich conditions. However, Kohan et al [42] and Van de Walle [43] challenged this conclusion in 2000 from different aspects. Kohan showed that both V_O and Zn_i theoretically had high formation energies in n-type ZnO, and therefore neither V_O nor Zn_i would exist in measurable quantities. Furthermore, it was also indicated that V_O and Zn_i were deep donors, so even if one or other were present, its ionization energy would be too high to produce free electrons. Although other theoretical analysis suggested that Zn_i was actually a shallow donor [44, 45], and had been proven by electron-irradiation experiments [46], the high formation energy of Zn_i mentioned earlier still limited its ability to contribute to n-type conductivity.

H.L. Ma and al said that: there are two reasons to explain the change of carrier mobility with T_S . On the one hand, the concentration of donor (V_O) increases with the rise of the T_S at a certain range. Hence, the scattering of carriers (V_O) is enhanced, which reduces the carrier mobility. On the other hand, the orientation of C-axis becomes stronger with increasing T_S . The probability of grain boundary scattering for the carriers moving parallel to the surface increases, and therefore, the mobility paralleled to the surface direction reduces [47].

I.5 The thin films alloys

I.5.1 MgO-ZnO alloys

ZnO is a large gap semiconductor, it is transparent in the visible and in the near infrared. It has a set of properties which allow its use in a certain number of applications such as for example a chemical sensor in thin layers [14].

To enhance the efficiency, the electronic structure, ZnO can be alloyed with MgO to form a ternary $Mg_xZn_{1-x}O$ compound, thus, enabling bandgap engineering and luminescence in the UV regime [15] Often, the combination of these group-II oxides in alloys leads to crystal structure mismatch: undoped ZnO prefers the hexagonal wurtzite (B4) structure or the fourfold coordinated zinc-blende structure (B3), while MgO favors the cubic rock salt (B1)

structure at ambient conditions.[16, 17] Experiments have shown that $Mg_xZn_{1-x}O$ exhibits the (B4) structure for high ZnO concentration,[18] while preferring the B1 structure at high MgO concentration.[19] At intermediate concentrations, it exhibits phase separation [20] due to its compositional gradient, which often leads to a thermodynamically unstable crystal structure. In general, the isovalent and isostructural II–VI alloys are thermodynamically unstable because the mixing enthalpy in either the B1, B3, or B4 structure is always positive.[20,21] The difficulty in synthesizing stable phases of MgO–ZnO alloys has hindered the adequate exploitation of their promising properties for technological applications. This prompted earlier calculations on the stability of the $Mg_xZn_{1-x}O$ alloy system.[20,22]

I.6 Elaboration methods of MgO-ZnO thin film

Thin films are generally used to enhance the surface properties of solids. Transmission, reflection, absorption, etc. permeation and electrical behaviour are only some of properties that can be improved by using a thin film. Thin film technologies are divided into PVD (Physical Vapour deposition) and CVD (Chemical Vapour deposition) processes (Table I.2).

Thin film of all materials created by any deposition technique exhibits different features such as:

- the beginning of a random nucleation process follows by nucleation and growth stages. These stages are dependent on deposition conditions.
- The nucleation stage can be modified significantly by external agencies, such as electron or ion bombardment.
- Film microstructure, associated defect structure, and film stress depend on the deposition conditions at the nucleation stage.
- The crystal phase and the orientation of the films are governed by the deposition conditions.

The basic properties of, such as film composition, crystal phase and orientation, film thickness, and microstructure, are controlled by the deposition conditions and methods.

The MgO-ZnO films have been deposited by various methods including molecular beam epitaxy [27], sol-gel process [28-31], successive ionic layer adsorption and reaction (SILAR) [32], ultrasonic spray pyrolysis (USP) [33,34], and ion beam assisted deposition [35].

Table I.2: Thin Film Deposition Techniques [36]

Thin Film Deposition techniques		
Physical Vapour Deposition (PVD)		Chemical Vapour Deposition (CVD)
Thermal Process	Athermal Process	
1)Thermal deposition	1) Direct current Diode sputtering	1) Thermally activated CVD
2)Electron Beam Deposition	2) Radio Frequency sputtering	2) Plasma Enhaanced CVD
3)Molecular Beam Epitaxy deposition	3) Magnetron sputtering	3)Photo-assisted CVD
4)Pulses Laser Deposition	4) Unbalanced Magnetron Sputtering	4) Metal organic CVD

I.6.1 Physical vapour Deposition (PVD)

Physical vapour Deposition technique is the transfer of atoms and molucules from a source to a substrate by a process that relies on physical methods to produce the vapour

species. Physical vapour deposition is carried out in high vacuum to avoid contamination of the film by ambient atmosphere [37].

I.6 .1.1 Molecular Beam Epitaxy (MBE):

This process is based on the deposition of thermal beam of atoms or molecules on a clean surface of a single-crystalline substrate held at high temperature under ultra high vacuum conditions to form an epitaxial film [38]. Figure I.2 shows a typical MBE system. MBE is a sophisticated and finely controlled method for growing single-crystal epitaxial films in high vacuum. Limitations of MBE are the expensive equipment and its complex operation [39]

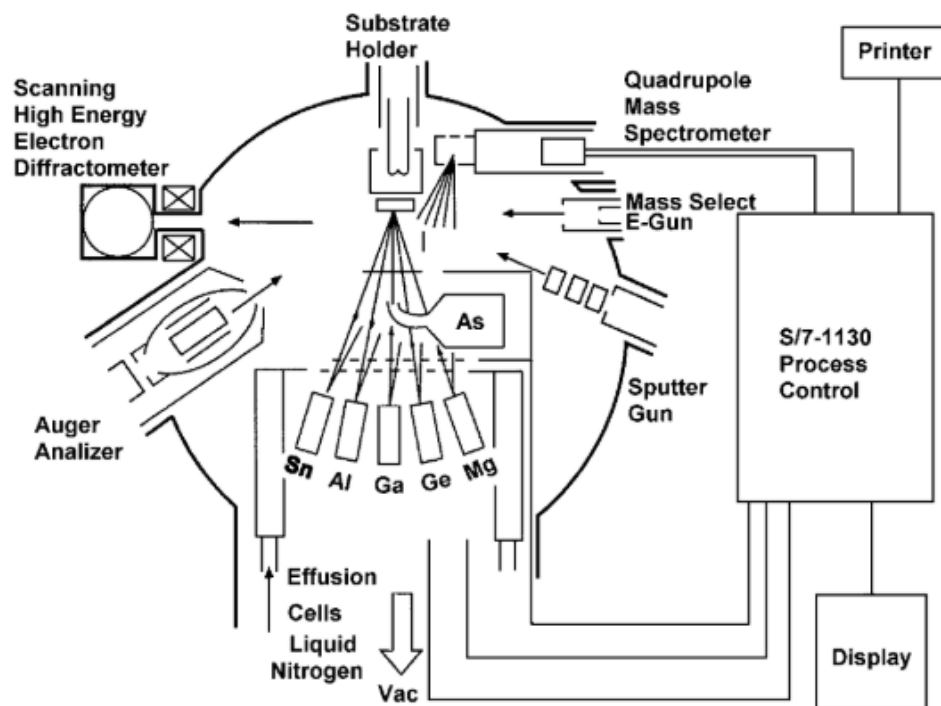


Fig I.2 : Molecule Bean Epitaxy (MBE) system.[38]

I.6.2 Chemical Vapour Deposition (CVD)

The process by which the non-volatile products of a gas phase reaction are allowed to deposit onto a substrate is known as chemical vapour deposition [39] the main feature of CVD

is its versatility for synthesizing both simple and complex compounds with relative ease. Fundamental principles of CVD encompass an interdisciplinary range of gas-phase reaction chemistry, thermodynamics, kinetics, transport mechanisms, film growth phenomena and reactor engineering [40]. The advantages of CVD include high deposition rate, low price and flexibility in composition control. However, due to high deposition temperature, CVD is not suitable for substrates which are thermally unstable at high temperatures[41]

I.7 Applications

The modification of the surface of a substrate permit to couple its properties and the properties of the surface material (deposited). The modification of the surface of a substrate gives it one or more additional physicochemical properties (resistance to corrosion, electrical insulation, etc.): the use of a low added value substrate leads to deduct manufacturing costs while having the required physical and chemical surface properties.

The first surface modifications had an aesthetic purpose (painting, gold plating ...) while more technical applications concerned metallurgy [ref].

During the 20th century, more sophisticated applications diversified in the following fields: [ref]

Microelectronics: it was able to develop from the 1960s through the implementation of layers becoming thinner conductive or insulating, and can be found subtypes passivating layer (electronic contact), PN junction, diode, transistor, material piezoelectric, LED lamp, superconductor,

Optic: while retaining the aesthetic applications, the optical applications of the layers were used to develop more effective radiation sensors, such as anti-reflection layers in solar cells, mirror glass, anti-reflection treatment of camera lenses, photo-detection , flat screen displays, ophthalmic applications, optical guide (energy controls - architecture, vehicles, energy conversion, etc.)

Mechanic: tribological coatings (dry lubrication, erosion, abrasion; diffusion barriers...)

Chemistry: the main applications of surface coatings are oriented towards better corrosion resistance by the creation of a waterproof film (corrosion resistance), gas sensor, catalytic coatings, protective layers,

Thermal: the use of a thermal barrier layer decreases for example the surface temperature of the metal of the fins of the reactors thus making it possible to improve the performances of the reactors (increase in the internal temperature),

Biology: biological micro sensors, biochips, biocompatible materials ...

Micro and nanotechnologies: mechanical and chemical sensors, microfluidics, actuators, detectors, adaptive optics, nano photonics...

Magnetic: information storage (computer memory), security devices, sensors ...

Decoration: watches, glasses, jewelry, home equipment, etc.

I.8 Conclusion

Magnesium oxide and Zinc oxide (MgO,ZnO) seems to have many interesting properties as MgO-ZnO thin films such as high electrical resistivity, high optical transparency, good chemical resistance, excellent thermal and thermodynamic stabilities, high secondary electron emission stability, low dielectric constant and low refractive index. These unusual properties caused that MgO-ZnO films have been widely used in a lot of applications.

REFERENCES:

[1] Mahadeva, S. K., Fan, J., Biswas, A., Sreelatha, K. S., Belova, L., & Rao, K. V. (2013). Magnetism of amorphous and nano-crystallized Dc-sputter-deposited MgO thin films. *Nanomaterials*, 3(3), 486-497.

[2] Feng, F., Zhang, X., Qu, T., Liu, B., Huang, J., Li, J., ... & Feng, P. (2018). Surface scaling analysis of textured MgO thin films fabricated by energetic particle self-assisted deposition. *Applied Surface Science*, 437, 287-293.

- [3] Chaouch, N., Benramache, S., & Lakel, S. (2020). Synthesis and Characterization of Physical Properties of MgO Thin Films by Various Concentrations. *Journal of Microelectronics and Electronic Packaging*, 17(1), 23-27.
- [4] Kim, S. G., Kim, J. Y., & Kim, H. J. (2000). Deposition of MgO thin films by modified electrostatic spray pyrolysis method. *Thin solid films*, 376(1-2), 110-114.
- [5] Ho, I. C., Xu, Y., & Mackenzie, J. D. (1997). Electrical and optical properties of MgO thin film prepared by sol-gel technique. *Journal of Sol-Gel Science and Technology*, 9(3), 295-301.
- [6] Kim, S. G., Kim, J. Y., & Kim, H. J. (2000). Deposition of MgO thin films by modified electrostatic spray pyrolysis method. *Thin solid films*, 376(1-2), 110-114.
- [7] Durusoy, H. Z. (1991). Growth structures of MgO films on Si (100) and Si (111) surfaces. *Journal of materials science letters*, 10(17), 1023-1025.
- [8] Hsu, W. Y., & Raj, R. (1992). MgO epitaxial thin films on (100) GaAs as a substrate for the growth of oriented PbTiO₃. *Applied physics letters*, 60(25), 3105-3107.]
- [9] Mihara, T., Mochizuki, S., & Makabe, R. (1996). c-Axis Oriented PbTiO₃ Thin Films on M]
- [M] Knözinger, H., & Kochloefl, K. (2000). Heterogeneous catalysis and solid catalysts. *Ullmann's Encyclopedia of Industrial Chemistry*.
- [11] Ropp, R. C. (2013). Chapter 5-Group 14 (C, Si, Ge, Sn, and Pb) Alkaline Earth Compounds. In *580 Encyclopedia of the Alkaline Earth Compounds*, Ropp, RC, Ed. Elsevier: Amsterdam, 581, 351-480.
- [12] Guo, X. L., Liu, Z. G., Chen, X. Y., Zhu, S. N., Xiong, S. B., Hu, W. S., & Lin, C. Y. (1996). Pulsed laser deposition of/MgO bilayered films on Si wafer in waveguide form. *Journal of Physics D: Applied Physics*, 29(6), 1632.
- [13] Raj, A. M. E., Jayachandran, M., & Sanjeeviraja, C. (2010). Fabrication techniques and material properties of dielectric MgO thin films—A status review. *CIRP Journal of Manufacturing Science and Technology*, 2(2), 92-113.

- [14] Saadeddin, I. (2007). Preparation and characterization of new transparent conducting oxides based on SnO₂ (indice) and In₂ (indice) O₃ (indice): ceramics and thin films (Doctoral dissertation, Bordeaux 1).
- [15] D. Jiang, C. Shan, J. Zhang, Y. Lu, B. Yao, D. Zhao, Z. Zhang, X. Fan, and D. Shen, *Cryst. Growth Des.* 9(1), 454–456 (2009).
- [16] D. C. Reynolds, D. C. Look, and B. Jogai, *Solid State Commun.* 99(12), 873–875 (1996).
- [17] O. Madelung, U. Rössler, and M. Schulz, *Landolt-Brnstein Database*, Vol. 10 (1999), see <http://www.springermaterials.com>
- [18] Y. Ohno, D. K. Young, B. Beschoten, F. Matsukura, H. Ohno, and D. D. Awschalom, *Nature* 402(6763), 790–792 (1999)
- [19] J. Narayan, A. Sharma, A. Kvit, C. Jin, J. Muth, and O. Holland, *Solid State Commun.* 121(1), 9–13 (2001)
- [20] M. Sanati, G. L. W. Hart, and A. Zunger, *Phys. Rev. B* 68, 155210 (2003).
- [21] X. F. Fan, H. D. Sun, Z. X. Shen, J.-L. Kuo, and Y. M. Lu, *J. Phys. Condens. Matter* 20(23), 235221 (2008);
- [22] Y.-S. Kim, E. C. Lee, and K. J. Chang, *J. Kor. Phys. Soc.* 39, 92 (2001).
- [23] Kohnke E.E, *Phys. Chem. Solids*, 23, 1557-1562, (1962)
- [24] K. Reimann and M., Steube, *Solid State Commun.*, 105, 649-652, (1998).
- [25] J. Maier and W. Goepel, *J. Solid State Chem.*, 72, 293-302, (1988).
- [26] M. Nagasawa, S. Shionoya, and S. Makishima, *Japan. J. Appl. Phys.*, 4, 195-202, (1965).
- [27] Niu, F., Hoerman, B. H., & Wessels, B. W. (2000). Metalorganic molecular beam epitaxy of magnesium oxide on silicon. *MRS Online Proceedings Library Archive*, 619.

- [28] Maiti, P., Das, P. S., Bhattacharya, M., Mukherjee, S., Saha, B., Mullick, A. K., & Mukhopadhyay, A. K. (2017). Transparent Al³⁺ doped MgO thin films for functional applications. *Materials Research Express*, 4(8), 086405.
- [29] Sharma, U., & Jeevanandam, P. (2015). Synthesis of Zn²⁺-doped MgO nanoparticles using substituted brucite precursors and studies on their optical properties. *Journal of Sol-Gel Science and Technology*, 75(3), 635-648.
- [30] Bazhan, Z., Ghodsi, F. E., & Mazloom, J. (2013). Effect of stabilizer on optical and structural properties of MgO thin films prepared by sol-gel method. *Bulletin of Materials Science*, 36(5), 899-905.
- [31] Demirci, S., Öztürk, B., Yildirim, S., Bakal, F., Erol, M., Sancakoğlu, O., ... & Batar, T. (2015). Synthesis and comparison of the photocatalytic activities of flame spray pyrolysis and sol-gel derived magnesium oxide nano-scale particles. *Materials Science in Semiconductor Processing*, 34, 154-161.
- [32] Güney, H., & İskenderoğlu, D. (2018). The effect of Ag dopant on MgO nanocrystallites grown by SILAR method. *Materials Science in Semiconductor Processing*, 84, 151-156.
- [33] Kurtaran, S., Akyuz, I., & Atay, F. (2013). Evaluation of optical parameters and characterization of ultrasonically sprayed MgO films by spectroscopic ellipsometry. *Applied surface science*, 265, 709-713.
- [34] Diachenko, O. V., Opanasiuk, A. S., Kurbatov, D. I., Opanasiuk, N. M., Kononov, O. K., Cheong, H., & Nam, D. (2016). Surface morphology, structural and optical properties of MgO films obtained by spray pyrolysis technique.
- [35] Stan, L., Arendt, P. N., DePaula, R. F., Usov, I. O., & Groves, J. R. (2006). Effect of substrate temperature on the texture of MgO films grown by ion beam assisted deposition. *Superconductor Science and Technology*, 19(4), 365.
- [36] Hariech, S. (2009). Elaboration et caractérisation des couches minces de sulfure de cadmium (CdS) préparées par bain chimique (CBD).
- [37] Seshan, K. (2001). *Handbook of thin film deposition processes and techniques*. William Andrew.

- [38] Wasa, K., Kitabatake, M., & Adachi, H. (2004). *Thin film materials technology: sputtering of control compound materials*. Springer Science & Business Media.
- [38] Bishop, C. (2011). *Vacuum deposition onto webs, films and foils*. William Andrew.
- [39] Pankove, J. I., & Moustakas, T. D. (1999). Semiconductors and semimetals: a treatise. Gallium Nitride (GaN) II.
- [40] Park, J. H., & Sudarshan, T. S. (Eds.). (2001). *Chemical vapor deposition* (Vol. 2). ASM international.
- [41] Gutfreund, H., Horovitz, B., & Weger, M. (1974). Peierls-Frohlich instability and superconductivity in linear chain crystals. *Journal of Physics C: Solid State Physics*, 7(2), 383.

CHAPTER II

EXPERIMENTAL

SECTION

II.1. Introduction

In this study, a new route to produce pure and composite ZnO-MgO thin films has been presented. In the process the pure ZnO thin films were the starting point, ending up with MgO by doping various concentration of Mg with the help of spray pyrolysis technique. The crystal phases in all doping levels have been obtained when the samples annealed at 450 °C. The X-ray diffraction spectra, the scanning electron microscopy micrographs and UV-Vis absorption spectra have been performed to elucidate the composed film structures.

II.2. Elaboration

The principle of the spray pyrolysis method (or spray pyrolysis or also pyrolytic spraying) consists in mechanically spraying a solution of precursors chemicals, containing the different constituents of the compound ZnO (zinc acetate and magnesium acetate $(\text{Mg}(\text{CH}_3\text{COO})_2 \cdot 4\text{H}_2\text{O})$) on substrates arranged on a substrate holder heated. After spraying the solution, a chemical reaction occurs on the hot surface (substrate), which provides a thin layer of ZnO-MgO after evaporation elements of the reaction (volatile elements).

In our work, we have studied the effect of concentration on the physical properties of the elaborated MgO-ZnO thin. The different layers were produced on glass substrates heated to temperature of 450 °C.

II.3. Spray pyrolysis technique (SPT)

Spray pyrolysis is a technique widely used to prepare materials in different forms: thin, thick, dense, porous and even deposits multilayer and ceramic coatings can be prepared using this technique [1]. The principle of this technique is based on the formation of droplets of a solution containing the different constituents of the compound transported by a flow to be deposited on a substrate heated by a heating system to temperatures appropriate (activation of the chemical reaction between compounds). Thus the solvent evaporates and the other elements react to form the final compound (hence the name pyrolysis: "pyro" for heat and "lysis" for decomposition). This experience may be carried out under a normal atmosphere [2].

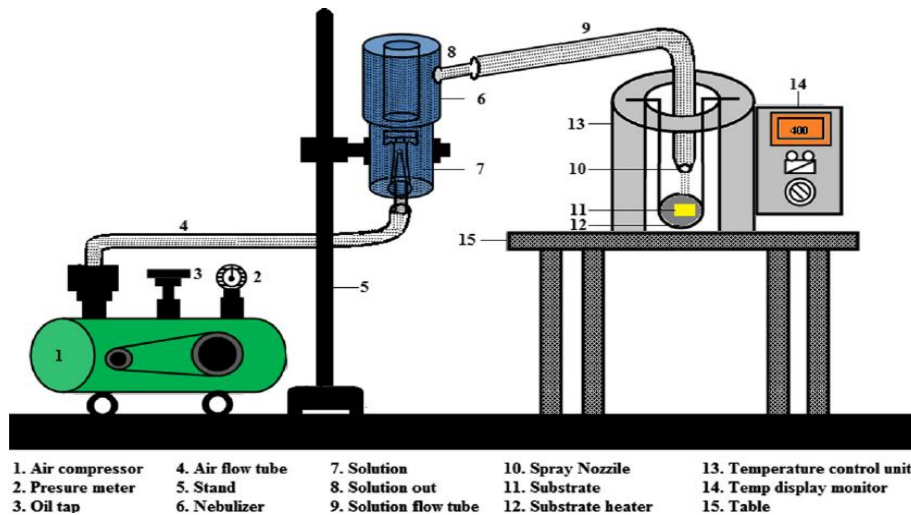


Figure II.1: Experimental diagram of the spray pyrolysis process [3].

II.4. The advantages of the spray pyrolysis technique

The droplet size is 5 μm ; it is $\approx 40 \mu\text{m}$ in the case of the ultrasonic spray and 30 μm for the sol-gel.

-It allows good control of the chemical composition of the material.

-We can use several products at the same time, in particular for doping [4].

II.5. Experimental procedure

II.5.1. Preparation of the substrate

The structural properties of the layer to be deposited are strongly linked to the nature of the substrate. Thus a thin layer of the same material, of the same thickness may have significantly different physical properties depending on whether it is deposited on a substrate amorphous insulator such as glass, a monocrystalline silicon substrate for example, or a conductive substrate such as ITO (indium tin oxide) [5].

II.5.1.1. Choice of deposition substrate

The choice of substrates is dictated by:

↪ **Adhesion:** The solution should adhere to the substrate.

↳ **Physical properties:** the physical properties of the substrates must be in agree with the type of study you want to conduct, for example:

- ❖ For the study of the optical properties of wave guiding it is imperative to choose a substrate with a refractive index lower than that of the material to be deposited [6].

Some applications require the use of conductive substrates such as ITO while others ask for insulating substrates like glass. In our work, we used glass substrates.

II.5.1.2. Cleaning of substrates

As we have mentioned, these substrates require special preparation in order that they serve as a support for the deposit.

Cleaning the substrates is a very important step which takes place in a place clean, because this step determines the qualities of adhesion and homogeneity of the layers filed.

The substrates must be free from grease, scratches and impurities such as dust. The procedure for cleaning the substrates that we have chosen is the following:

- Soap cleaning
- Rinsing with distilled water
- Cleaning with methanol
- Finally, drying with an optical paper [7].

II.5.2. Preparation of the solution

In this work we used the following precursors: zinc acetate ($C_4H_6O_4Zn \cdot 2H_2O$), as source material which we dissolved in water, we get $[ZnO] = 0,1 \text{ mol/l}$, and we dissolve mannesium acetate ($Mg(CH_3COO)_2 \cdot 4H_2O$) in water, we obtain $[MgO] = 0,1 \text{ mol/l}$.

We take 70 ml of Mgo and 30 ml of ZnO, then stir for 2 hours to obtain a homogeneous solution.

Table II.1: The experimental conditions for the production of ZnO-MgO thin films.

Precursors	Concentration of solution M	La masse	T C°
Zinc acetate (C ₄ H ₆ O ₄ Zn.2H ₂ O)	0,1	1.363 g	450C°
Magnesium acetate (Mg(CH ₃ COO) ₂ • 4H ₂ O)	0,1	2.032 g	

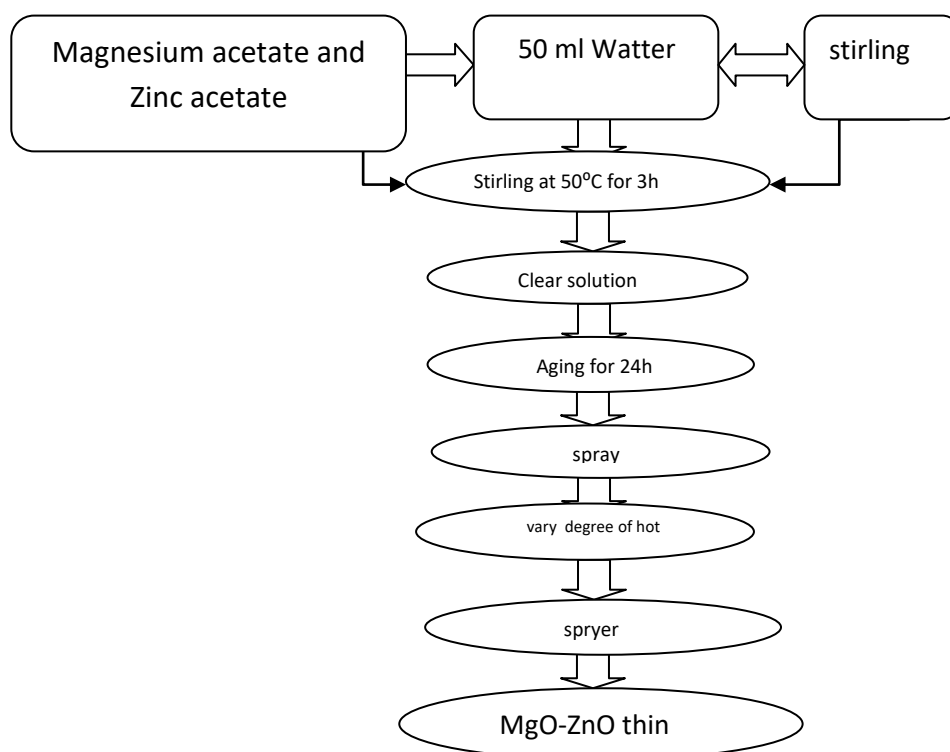


Figure II.2 Flow chart of Spray pyrolysis method for preparation of MgO-ZnO thin films.

II.5.3. Preparation of the substrate

A) Glass Substrates

During this study, spray pneumatic MgO-ZnO thin films were deposited on glass substrates (see Figure II.2). Which have a length of 2.5cm and a width of 2.5cm the choice of glass for these reasons:

- The thermal compatibility with MgO and ZnO (thermal dilation coefficients are $\alpha_{\text{glass}} = 8.5 \times 10^{-6} \text{ K}^{-1}$, to minimize the constraints with the interface film/substrate,
- For their transparency which adapts well for the optical characterization of films in the visible one.
- For economic reasons.

In order to obtain good adherence and uniformity for the films.



Figure II.3 Glass Substrates

B) Substrate Cleaning Process

The adherence and the quality of the depot repose on purity and the state on substrate thus the cleaning of the substrate is one of the most important steps to remove any contaminated organic compounds, the cleaning of our substrates surfaces is as follows:

- The substrates are cut using a pen with diamond point.
- Washing with soap solution to clean any dusts or attachments.
- Washing with distilled water to remove soap, and then with acetone during 2 min.
- Rinsing with distilled water again.

- Washing with ethanol during 2 min at ambient temperature.
- Cleaning in water distilled bath.

II.6. Thin Film Deposition

The deposition procedure comes immediately after the preparation of the substrates and solutions and is presented in several stages:

The substrates are placed above a substrate holder and to avoid thermal shock from substrates the substrate holder is gradually heated from room temperature gradually up to the temperature chosen for the deposits (450 ° C). Very droplets fines are sprayed onto the heated substrate which causes, by pyrolysis, the activation of the chemical reaction between the compounds, the solvent evaporates due to the reaction endothermic of the two compounds forming the thin layer. At the end of the deposit process, we stop heating and allow the substrates to cool above the substrate holder until the ambient temperature, in order to avoid thermal shocks which risk breaking the glasses, and then we collect our samples (Table 2).

Table II.2: Preparation of solutions at different constration

N°	MgO	ZnO	MgO-ZnO	T C°
S₁	0%	100%	20 ml(ZnO)	450 C°
S₂	30%	70%	6 ml(MgO) + 14 ml (ZnO)	
S₃	50%	50%	10 ml(MgO) + 10 ml (ZnO)	
S₄	70%	30%	14 ml (MgO) + 6 ml (ZnO)	
S₅	100%	0%	20 ml (MgO)	

II.6.1. Characterization of the films:

The microstructure, electrical and optical properties of **Magnesium acetate and Zinc acetate** thin films were evaluated using different characterization techniques such as:

- Ultraviolet visible spectroscopy, for the determination of transmittance and the optical gap and the refraction index of films.
- The electrical characterization was measured the electrical conductivity by the mean of four points.

A brief introduction for each characterization technique will be provided in the following section.

II.6.2. Structural characterizations

This study made by X-ray diffraction aims to specify the structure and the crystallographic growth directions of the layers, to measure the parameters of mesh size and crystallite size. It should also make it possible to examine the state of the constraints in the depots

II.6.3. Electrical Conductivity Measurement:

The four-point probe is a very versatile device used widely for the investigation of electrical phenomena. The effect of the contact resistance could be eliminated with the use of such configuration. The most common in-line configuration has been adopted in this work (see figure II-5).

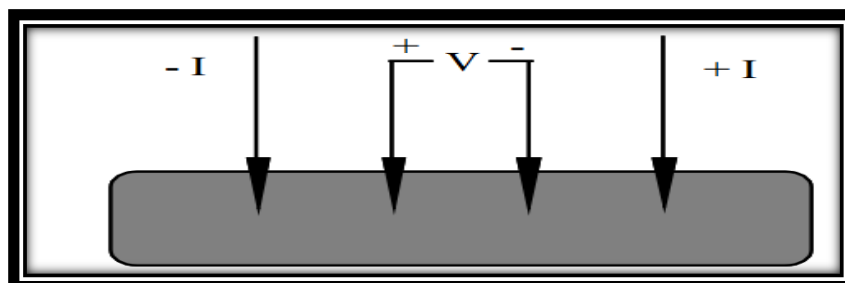


Figure II-4: Schematic of in-line four-point probe configuration

In the measurement, the four metal tips have been attached to the test sample. A high impedance current source of $I = 0.5 \mu\text{A}$ has been used to supply current through the outer two probes; a voltmeter measured the voltage V across the inner two probes. The probe spacing was 1 mm. Consequently, the sheet resistance of the film is derived from the formula [3]:

$$R_S = \frac{\pi}{\ln 2} * \frac{V}{I} \quad (\text{II.1})$$

where the factor of $\pi/\ln 2$ is on account of the effect of the current extending. If the film thickness is known, the resistivity is readily obtained from [3]:

$$\rho = R_S * d \quad (\text{II.2})$$

where d is the film thickness. The mean value of three measurements has been taken in order to reduce the measuring error [4].



Figure II. 5 Experimental dispositif.

II.6.4. Optical characterization

The optical techniques which characterize thin films are numerous such as:

- A) **Visible spectroscopy:** Is a technique based on the interaction of electromagnetic radiation and matter in the near UV to very near range IR. This technique makes it possible to determine the optical constants of the material studied (the rate transparency, the absorption coefficient, the optical gap and the extinction coefficient) [8].



Fig II.6 : Ultraviolet-visible spectrophotometer [9]

B) Principle of ultraviolet-visible absorption

Principle of UV-Visible Spectroscopy. The Principle of UV-Visible Spectroscopy is based on the absorption of ultraviolet light or visible light by chemical compounds, which results in the production of distinct spectra. Spectroscopy is based on the interaction between light and matter [10].

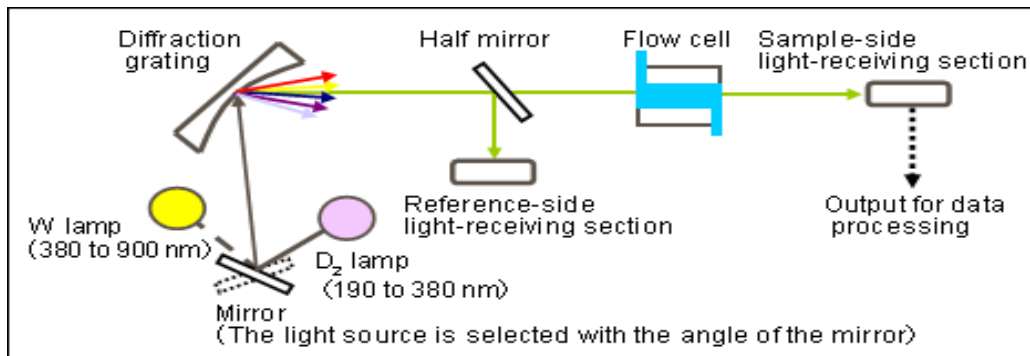


Figure II. 7 : The principle of operation of UV-visible

II.7. Conclusion

In this chapter we have presented the deposition and characterization technique adopted in our study. We recalled the principle of spray deposition and then presented the deposition system that we carried out in the laboratory, after we described the different characterization techniques used to analyze and determine the different optical and electrical properties of the films produced.

References

- [1] M. A. Herman, H. Sitter, and W. Richter. Epitaxy: Physical Principles and Technical Implementation. Springer-Verlag, 2010.
- [2] Pier Carlo Braga, Davide Ricci, “ Atomic Force Microscopy: Biomedical Methods and Applications”, Humana Press, New Jersey (2008)
- [3] Yiping Zhao, Gwo-Ching Wang, Toh-Ming Lu, “ Characterization of Amorphous and Crystalline Rough surface: Principles and Applications”, Academic Press, USA (2011)
- [4] Esther Belin-Ferré , “Surface Properties and Engineering of Complex Intermetallics” World Scientific Publishing Co. Pte. Ltd., Singapore (2010)
- [5] Baghezza M .Optical and electrical prpoprities of MgO thin films. Final Dissertation in Master.Biskra (2019)
- [6] Al. Boileau, These Ph.D, 2013, Université de Lorraine, France.
- [7] Walter Umrath. Fundamentals of vacuum technology. Technical report, Oerlikon Leybold Vacuum, 2007.
- [8] S. Abdullahi, M. Momoh, A.U Moreh, A.M. Bayawa, M. B. Abdullahi and I. Atiku, (2017) .Comparative Studies on Thin Film of Zinc Oxide (ZnO) Deposited by Spray

Pyrolysis and RF Sputtering Technique. Department of Physics, Usmanu Danfodiyo University Sokoto, Nigeria. ISSN 2321-435X

- [9] Waqar Ahmed, Mark J. Jackson, "Emerging nanotechnologies for manufacturing", Elsevier Inc., UK (2009)
- [10] Pier Carlo Braga, Davide Ricci, "Atomic Force Microscopy: Biomedical Methods and Applications", Humana Press, New Jersey (2014)

CHAPTER III

RESULTS AND

DISCUSSION

III.1. Introduction

Zinc oxide (ZnO) is one of the metal oxides and it is very free from harm to humans and the environment, and it is one of the most important oxides widely used in all scientific and technological applications because of its high transparency and good electrical conductivity. However, transparent conductive of ZnO thin films have been attracted significant attention in optoelectronic and piezoelectric devices [1]. Among these applications, MgO is appropriate for UV photodetectors and n-type electrical conductivity [2]. ZnO has been intensively studied as a promising material for organic solar cells because of its wide bandgap in the range of 3.3 – 3.4 eV, and high stability that are similar to NiO [3].

The aim of this work is to obtain a thin film with good physical characterizations for photovoltaic applications. We have prepared the MgO-ZnO thin films on the glass substrates using a spray pneumatic technique, the films were prepared at several rate solutions of MgO-ZnO are (0%+100%), (30%+70%), (50%+50%), (70%+30%), (100%+0%) of MgO-ZnO at a deposition temperature of 450 °C. The effect of rate solutions of MgO-ZnO on optical, electrical and structural characterizations has been studied.

III.2 Experimental procedure

Figure III.1 presents the protocol of the experimental setup for deposit MgO-ZnO thin films [4-6], which was based on the spraying MgO-ZnO solution on a heated glass substrate at 450 °C. In this work, we have fixed the distance between the heated glass substrate and the spray solution in the gun nozzle to 3.5 cm. then we have studied the effect of rate solutions of MgO-ZnO on optical, electrical and structural characterizations has been studied.

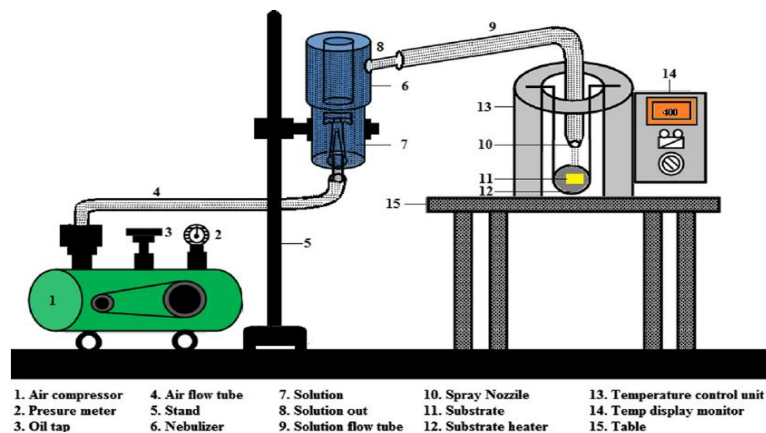


Figure III.1: Experimental diagram of the spray pyrolysis process..

ZnO spray solutions have been obtained by dissolving the powder of $(\text{Zn}(\text{CH}_3\text{COO})_2 \cdot 2\text{H}_2\text{O})$ in the absolute ethanol solution (99.995%) purity, for stabilization we have added drops of NaOH solution into the mixture solution of ZnO, then stirred for 180 min at 50 °C to the transparent solution (see Table III.1).

MgO spray solutions have been obtained by dissolving the powder of $(\text{Mg}(\text{CH}_3\text{COO})_2 \cdot 4\text{H}_2\text{O})$ in the absolute ethanol solution (99.995%) purity, for stabilization we have added drops of NaOH solution into the mixture solution of MgO, then stirred for 240 min at 30 °C to the transparent solution (see Table III.1).

Table III.1: The experimental conditions for the production of ZnO-MgO thin films.

Precursors	Concentration of solution M	La masse	T C°
Zinc acetate ($\text{C}_4\text{H}_6\text{O}_4\text{Zn} \cdot 2\text{H}_2\text{O}$)	0,1	1.363 g	450C°
Magnesium acetate ($\text{Mg}(\text{CH}_3\text{COO})_2 \cdot 4\text{H}_2\text{O}$)	0,1	2.032 g	

The MgO-ZnO thin films have been characterized in order to get the physical properties such as optical, structural and electrical. The crystalline structure of fabricated films were obtained by X-ray diffraction (Bruker-XRD AXS-8D, $\lambda\text{CuK}\alpha = 0.15406$ nm with 2θ varying between 20 ° and 80 °). The optical transmittance of fabricated ZnO thin films was measured by an UV-visible (35-LAMBDA UV) in the range of 300–900 nm. All characterizations have been made at stable conditions. All measurements were required at room temperature (RT).

III. 3 The structural characterizations

The analytical results of X-ray diffraction of fabricated MgO-ZnO thin films grown at several MgO-ZnO spray solutions are shown in Figure III.2. The fabricated MgO and ZnO with 0.1 M (see Figure III.2). We have observed a different crystal peaks that could be detected in the fabricated thin film, it was identified as (002) and (102) crystal peaks for the ZnO phase at diffraction angle are 34.51 and 36.36° respectively [7], the film exhibit a polycrystalline of the hexagonal wurtzite structure of ZnO, the preferred orientation of c-axis was observed for (002) crystal plane. However, it was observed as (111), (200), (102) and (311) crystal peaks for the MgO phase at diffraction angle are 38.1, 47.4, 63.4 and 73.3° respectively [8]. Moreover we have observed a another phases of MgO it are MgOH and $\text{Mg}(\text{OH})_2$.

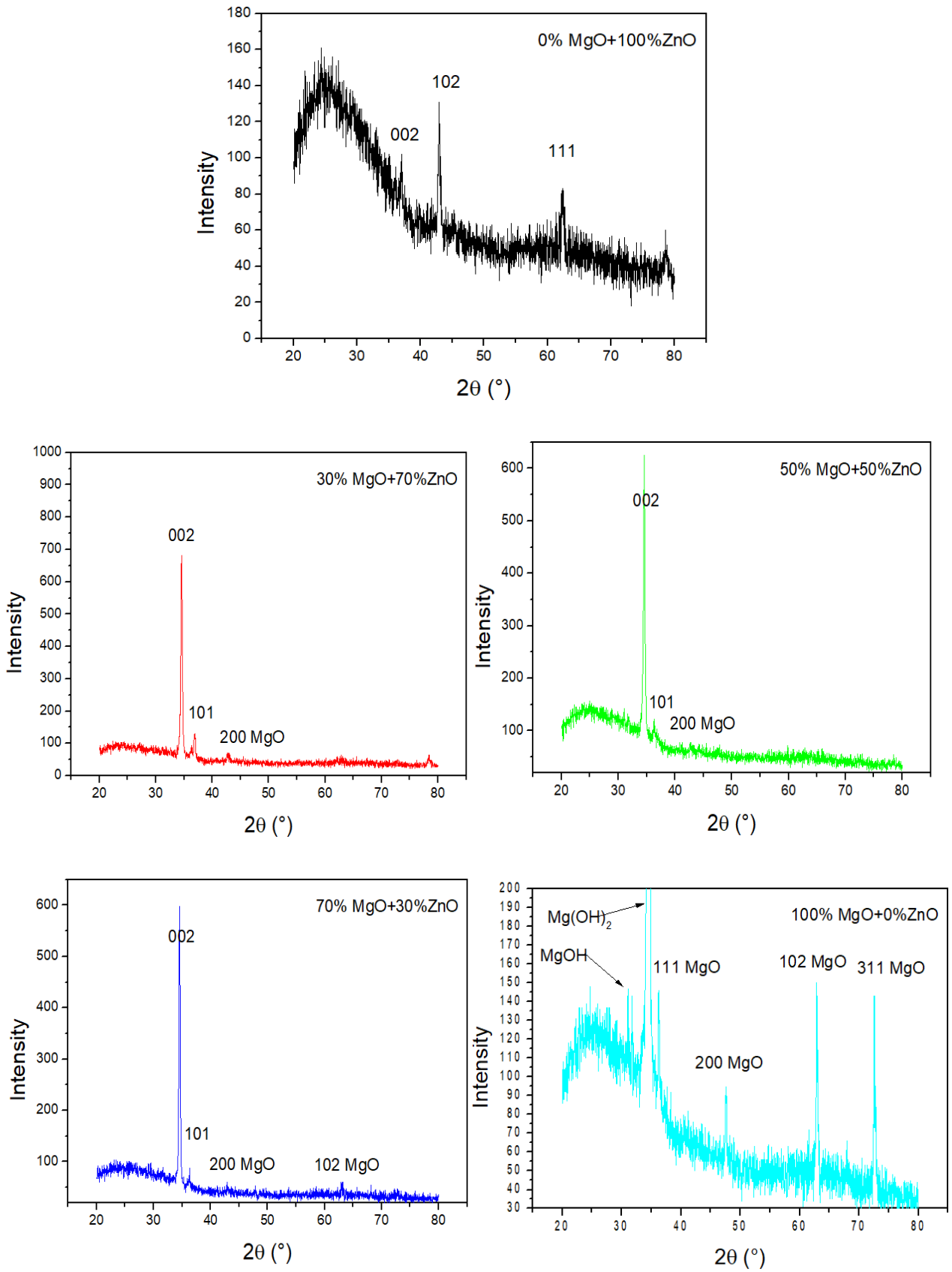


Figure III. 2 the XRD spectrum of MgO-ZnO thin films deposited at several MgO and ZnO spray solutions.

The detailed of crystalline structure information of fabricated ZnO thin films was presented to calculate the grain size of fabricated ZnO thin films. The Grain size $G_{(002)}$ was determined by applying the Scherer's equation [9]:

$$G = \frac{0.9\lambda}{\beta \cos\theta} \quad (1)$$

Where θ , β , λ and G are the diffraction angle of the crystal peak, FWHM, the longer of the X-ray wavelength, and the measured grain size, respectively.

The average mean strain for the lattice along the a and c-axis in the randomly oriented has been estimated from the lattice parameters using the equal below [10-14]:

$$\varepsilon = \frac{c - c_0}{c_0} \times 100\% \quad (2)$$

$$\varepsilon = \frac{a - a_0}{a_0} \times 100\% \quad (3)$$

Where ε is the mean stress of deposited thin films (see Tables III.2 and III.3), a and C the lattices constant of MgO and ZnO thin films, respectively, And a_0 and C_0 the lattice constant of bulk (standard).

The variation of the grain size, Bragg angle, the full width at half-maximum FWHM, lattice parameters C and a , and the strain ε crystal plane were measured as a function of rate solutions of fabricated MgO-ZnO thin films at several MgO and ZnO solution precursor molarities, it are presented in Tables III.2 and III.3, the measured grain size of ZnO thin films was increased with decreasing ZnO solutions in the final solution. And the grain size of MgO increased with increasing the MgO solution.

Table III.2 Bragg angle 2θ , the full width at half-maximum FWHM β , the grain size G , lattice parameters C and a , and the strain \mathcal{E} for (0 0 2) crystal plane of ZnO were measured as a function of rate solutions.

rate solutions	2θ (deg)	β (deg)	G (nm)	C (A°)	a (A°)	\mathcal{E} (%)
0%MgO+100% ZnO	35.2	0.421	19.9	5.0111	3.312	-0.11
30%MgO+70% ZnO	34.7	0.129	65.1	5.0253	3.272	-0.03
70%MgO+50% ZnO	34.8	0.121	69.4	5.0284	3.268	+0.04
70%MgO+30% ZnO	34.9	0.110	76.2	5.0291	3.245	+0.07
100%MgO+0% ZnO	-	-	-	-	-	-

Table III.3 Bragg angle 2θ , the full width at half-maximum FWHM β , the grain size G , lattice parameters C and a , and the strain \mathcal{E} for (200) crystal plane of MgO were measured as a function of rate solutions.

rate solutions	2θ (deg)	β (deg)	G (nm)	C (A°)	a (A°)	\mathcal{E} (%)
0%MgO+100% ZnO	-	-	-	-	-	-
30%MgO+70% ZnO	48.15	0.425	19.75	-	4.213	-0.011
70%MgO+50% ZnO	48.15	0.388	21.63	-	4.238	+0.025
70%MgO+30% ZnO	48.15	0.364	23.23	-	4.321	+0.036
100%MgO+0% ZnO	48.15	0.347	24.17	-	4.334	+0.084

III. 4 The Optical characterizations

The optical transmission of fabricated MgO-ZnO thin films was determined as a function of longer of the wavelength is presented in Figure III3 shows the optical transmission of fabricated MgO-ZnO thin films obtained at several MgO and ZnO solution, the thin films were fabricated at low substrate temperatures is 450 °C. As can be seen, in the visible region the transmission of the thin films is about 80%. Figure III.4 show the absorbance variation of MgO-ZnO thin films obtained at several MgO and ZnO solution.

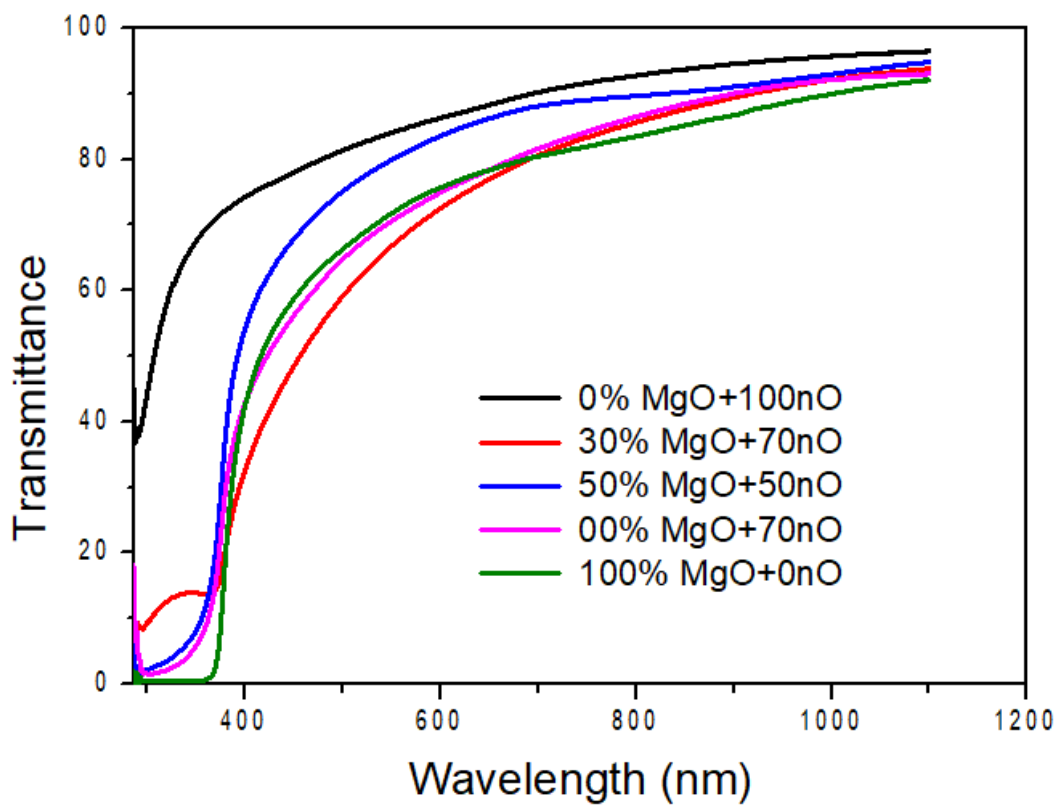


Figure III.3 Optical transmission of fabricated MgO-ZnO thin films at MgO and ZnO spray solutions.

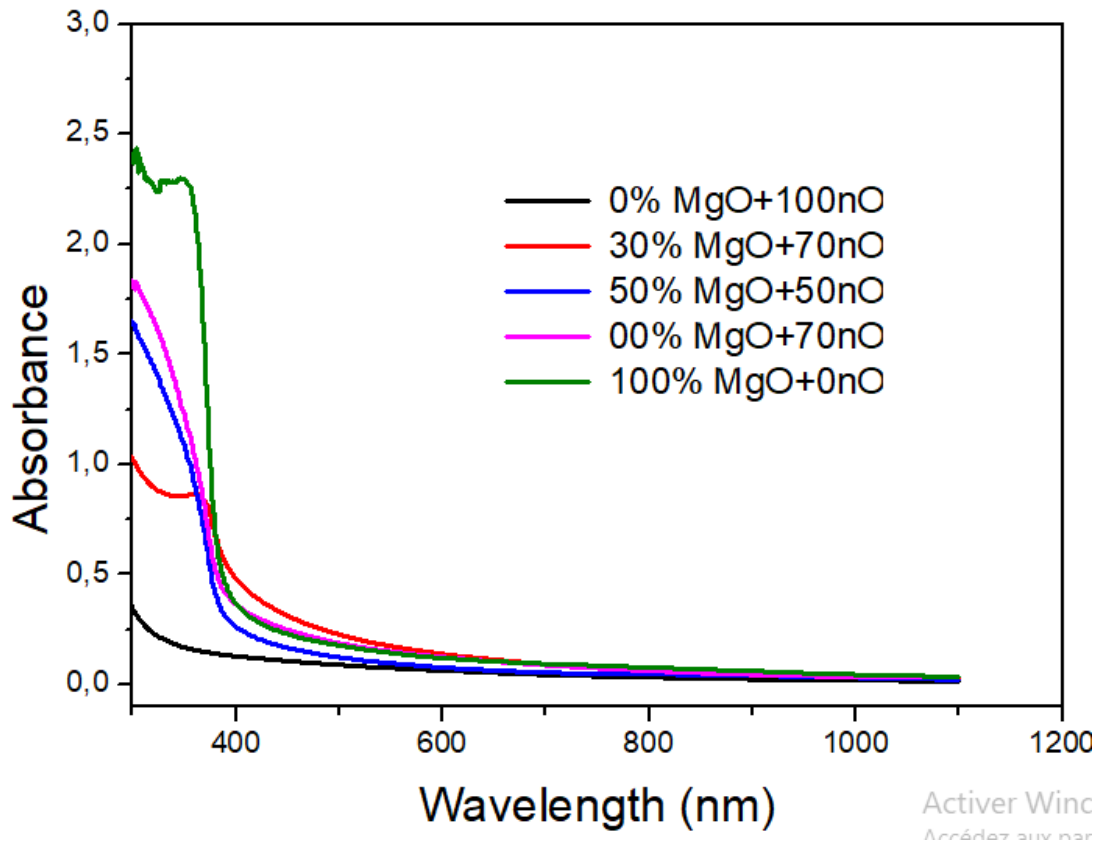


Figure III.4 Optical Absorbance of fabricated MgO-ZnO thin films at MgO and ZnO spray solutions.

The band gap energy (see figure III.5) of fabricated the thin films have been derived from the direct transitions of inter-band in the valence band and conduction band, it was determined by following equation [2-5,14]:

$$(Ah\nu)^2 = C(h\nu - E_g) \quad (4)$$

where A is the absorbance, C is a constant, $h\nu$ is the photon energy and E_g is the band gap energy of the thin films. However, the tail width can be calculated using the Urbach energy (see figure III.6) for the absorption coefficient at lower photon energy [7,8, 15,16]:

$$A = A_0 \exp\left(\frac{h\nu}{E_u}\right) \quad (5)$$

where A_0 and E_u are a constant and the Urbach energy of thin films.

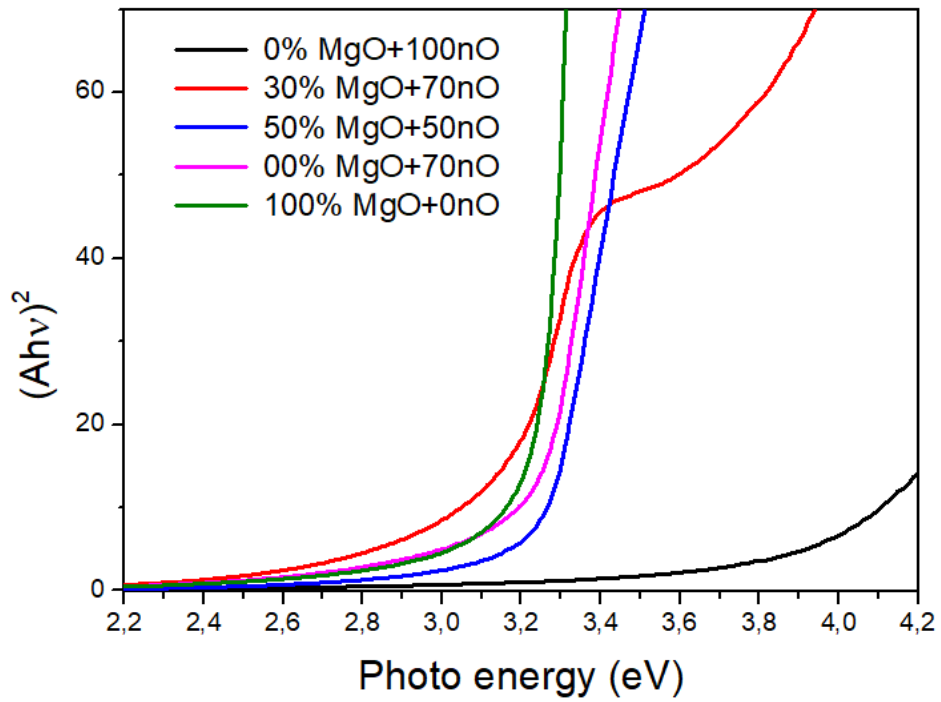


Figure III.5 Variation of $(Ah\nu)^2$ for measurements of the band gap energy

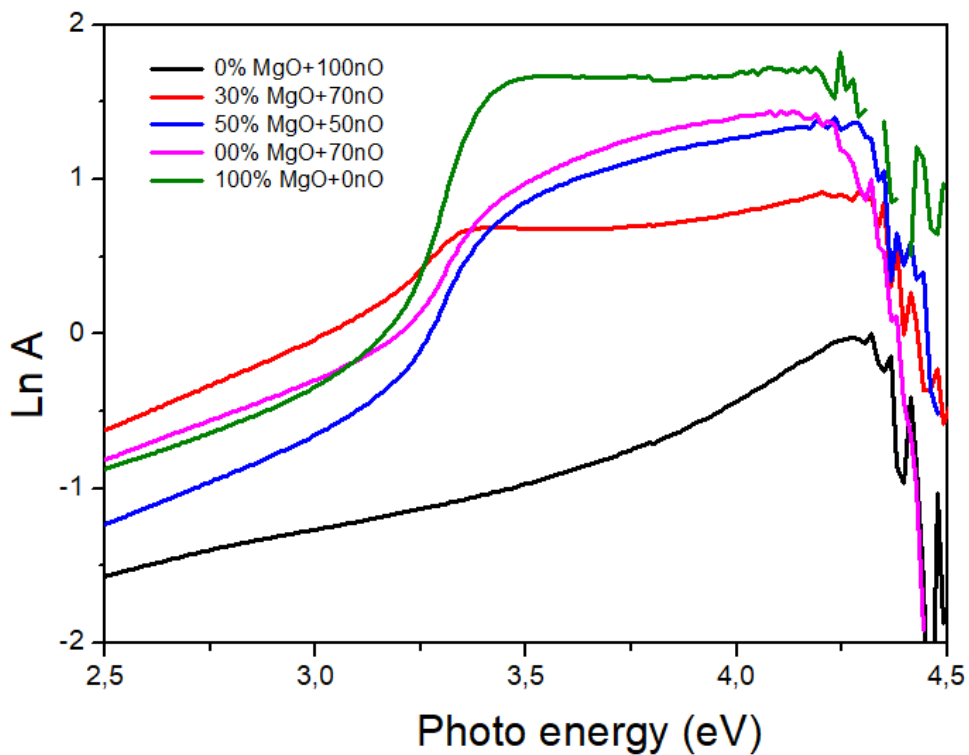


Figure III.6 Variation of $\text{Ln } A$ for measurements of the Urbach energy.

Reported in Figure III.7 the variation of the band gap energy E_g and Urbach energy E_u at several additions of MgO solutions, as seen, we note that the higher the MgO, the values are opposite caused by the absorption region, which is greatly decreased in this region. We have obtained good band gap energy and lowest Urbach energy for the thin film fabricated 100% MgO and 0% ZnO, which were 3.23 eV and 155 meV, respectively (see Table III.4). The decrease of the band gap energy with the decrease of the Urbach energy can be explained by the decrease of the defects, this attribution was obtained in the increase of the grain size (see Tables III.2 and III.3).

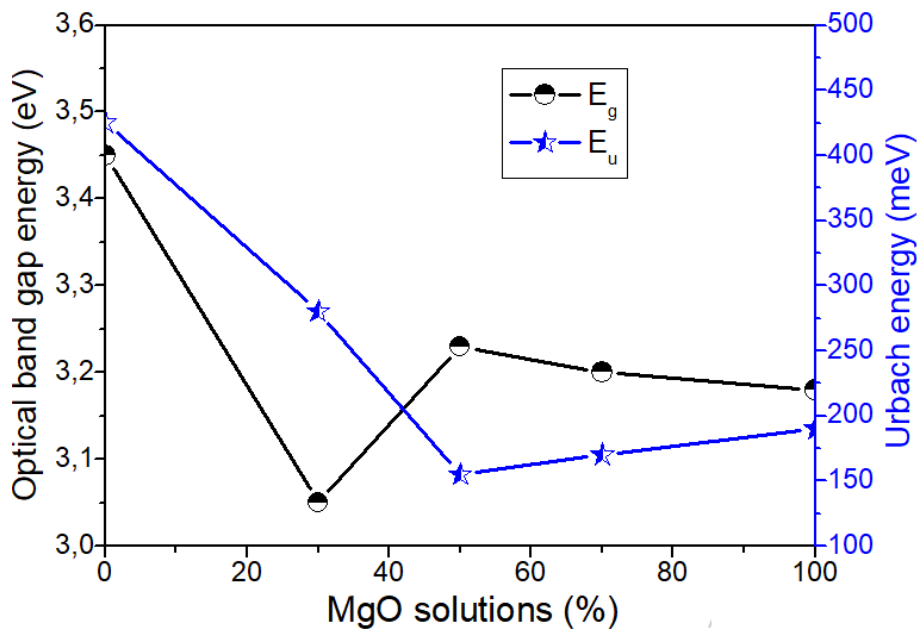


Figure III.7 Variation of bandgap energy and Urbach energy of fabricated MgO-ZnO thin films at several addition MgO solutions.

Table III.4 Variation of bandgap energy and Urbach energy of fabricated MgO-ZnO thin films at several addition MgO solutions.

rate solutions	Eg (Ev)	Eu 5meV)
0%MgO+100% ZnO	3.45	425
30%MgO+700% ZnO	3.05	280
70%MgO+50% ZnO	3.23	155
70%MgO+30% ZnO	3.20	170
100%MgO+0% ZnO	3.18	190

III.5 Conclusion

In this work, MgO-ZnO thin films were successfully fabricated on the heated glass substrates using a spray pneumatic method with several MgO and ZnO solutions of (0%+100%), (30%+70%), (50%+50%), (70%+30%), (100%+0%) of MgO-ZnO. The fabricated MgO-ZnO thin films have a good crystalline structure. The average transmission is about of 80 % in the visible region. We have obtained good band gap energy and lowest Urbach energy for the thin film fabricated 100% MgO and 0% ZnO, which were 3.23 eV and 155 meV, respectively (see Table III.4). The decrease of the band gap energy with the decrease of the Urbach energy can be explained by the decrease of the defects, this attribution was obtained in the increase of the grain size (see Tables III.2 and III.3).

References

- [1] A. Diha, S. Benramache, L. Fellah, J. Nano- Electron. Phys. 11 (2019) 03002.
- [2] S Benramache, B Benhaoua, Open Physics 14 (2016) 714-720
- [3] X. Fu, Z. Song, G. Wu, J. Huang, X. Duo, C. Lin, 16, 277–281 (1999)
- [4] M. C. Paganini, M. Chiesa, F. Dolci, P. Martino, E. Giamello, J. Phys. Chem. B 110, 11918 (2006).
- [5] J. Kramer, W. Ernst, C. Tegenkamp, H. Pfnür, Surf. Sci. 517,87 (2002); J. Kramer, C. Tegenkamp, H. Pfnür, Phys. Rev. B 67, 235401 (2003).
- [6] H. M. Benia, P. Myrach, N. Nilius, H.-J. Freund, Surf. Sci. 604, 435 (2010).
- [7] S. Benedetti, H.M. Benia, N. Nilius, S. Valeri, H.J. Freund, Chem. Phys. Lett. 430, 330 (2006)
- [8] A.M.E. Raj, V.B. Jothy, C. Ravidhas, T. Som, M. Jayachandran, C. Sanjeeviraja, Radiat. Phys. Chem. 78, 914–921 (2009)
- [9] V. Dhanasekaran, T. Mahalingam, J.-K. Rhee, J.P. Chu, Optik 124, 255–260 (2013)
- [10] R. Chandramohan, V. Dhanasekaran, S. Ezhilvizhian, T.A. Vijayan, J. Thirumalai, A. John Peter, T. Mahalingam, J. Mater. Sci. Mater. Electron. 23, 390–397 (2012)
- [11] G. Ertl, H. Knozinger, J. Weitkamp (eds.), Handbook of heterogenous catalysis. 4, Wiley–VCH, Weinheim, 2111 (1997)
- [12] A. Sanchez et al., J. Phys. Chem. A 103, 9573 (1999); H. Häkkinen, S. Abbet, A. Sanchez, U. Heiz, U. Landman, Angew. Chem. Int. Ed. 42, 1297 (2003); B. Yoon et al., Science 307, 403 (2005).

- [13] Pryds N, Cockburn D, Rodrigo K, Rasmussen IL, Knudsen J, Schou J.: *Appl Phys A* 2008, 93: 705–710. 10.1007/s00339-008-4700-2
- [14] Paranjpe A, IslamRaja M: *J Vac Sci Technol B* 1995, 13: 2105–2114.
- [15] Chen, WC., Peng, CY. & Chang, L. *Nanoscale Res Lett* (2014) 9: 551.
- [16] P.K. Samanta, M. Das, N.K. Rana, *J. Nano- Electron. Phys.* 11 (2019) 01028.

GENERAL

CONCLUSION

General Conclusion

In conclusion, highly transparent MgO-ZnO thin films have been deposited on glass substrate by spray pneumatic method. The influence of MgO and ZnO solutions on optical and structural properties was investigated.

In this work, MgO-ZnO thin films were successfully fabricated on the heated glass substrates using a spray pneumatic method with several MgO and ZnO solutions of (0%+100%), (30%+70%), (50%+50%), (70%+30%), (100%+0%) of MgO-ZnO.

The fabricated MgO-ZnO thin films have a good crystalline structure. The average transmission is about of 80 % in the visible region. We have obtained good band gap energy and lowest Urbach energy for the thin film fabricated 100% MgO and 0% ZnO, which were 3.23 eV and 155 meV, respectively. The decrease of the band gap energy with the decrease of the Urbach energy can be explained by the decrease of the defects, this attribution was obtained in the increase of the grain size (see Tables III.2 and III.3).

The best estimated optical and electrical characterisation MgO-ZnO thin films are achieved in prepared MgO-ZnO thin films with 70%+30% respectively.

ABSTRACT: Study the effect of concentration on the physical properties of the elaborated MgO-ZnO thin film

In this study, a new route to produce pure and composite ZnO-MgO thin films has been presented. In the process the pure ZnO thin films were the starting point, ending up with MgO by doping various percentages (from 0% to 100%) of Mg with the help of the spray pyrolysis method . The crystal phases in all doping levels have been obtained when the samples annealed at 450°C for a duration of 1 hours. The X-ray diffraction (XRD) spectra, the scanning electron microscopy (SEM) micrographs and UV-Vis absorption spectra have been performed to elucidate the composed film structures.

Mots clés : Zinc oxide (ZnO) - Magnesium oxide (MgO) - Spray ultrasonique - Concentration de la solution - Temperature de substrat - Pourcentage d'étain - Temperature de recuit.

ملخص : دراسة تأثير التركيز على الخواص الفيزيائية للطبقة الرقيقة MgO-ZnO المطورة .

في هذه الدراسة ، تم تقديم طريق جديد لإنتاج أغشية ZnO-MgO الرقيقة النقية والمركبة. في هذه العملية ، كانت أغشية ZnO الرقيقة النقية هي نقطة البداية ، وانتهت مع MgO عن طريق تعاطي المنشطات بنسب مختلفة (من 0% إلى 100%) من Mg بمساعدة طريقة الانحلال الحراري بالرش. تم الحصول على الأطوار البلورية في جميع مستويات المنشطات عند تلدين العينات عند درجة حرارة 450 درجة مئوية لمدة ساعة واحدة. تم إجراء أطياف حيود الأشعة السينية (XRD) والميكروسكوبات المجهرية للمسح الإلكتروني (SEM) وأطياف امتصاص UV-Vis لتوضيح هيكل الفيلم المكونة.

الكلمات المفتاحية :

أكسيد الزنك (ZnO)، أكسيد المغنيسيوم (MgO) ، الرش فوق صوتي ، تركيز المحلول ، درجة حرارة المسند ، نسبة التصدير ، درجة حرارة التلدين .